HHS Public Access

Author manuscript

Neurochem Int. Author manuscript; available in PMC 2018 December 01.

Published in final edited form as:

Neurochem Int. 2017 December ; 111: 69–81. doi:10.1016/j.neuint.2016.08.003.

Systemic administration of cell-free exosomes generated by human bone marrow derived mesenchymal stem cells cultured under 2D and 3D conditions improves functional recovery in rats after traumatic brain injury

Yanlu Zhang, MS, MD[1], **Michael Chopp, PhD**[2,3], **Zheng Gang Zhang, MD, PhD**[2], **Mark Katakowski, PhD**[2], **Hongqi Xin, PhD**[2], **Changsheng Qu, MD**[1], **Meser Ali, PhD**[4], **Asim Mahmood, MD**[1], and **Ye Xiong, MD, PhD**[1]

[1]Department of Neurosurgery, Henry Ford Hospital, Detroit, MI, USA

[2]Department of Neurology, Henry Ford Hospital, Detroit, MI, USA

[3]Department of Physics, Oakland University, Rochester, MI, USA

[4]Department of Radiology, Henry Ford Hospital, Detroit, MI

Abstract

Multipotent human bone marrow derived mesenchymal stem cells (hMSCs) improve functional outcome after experimental traumatic brain injury (TBI). The present study was designed to investigate whether systemic administration of cell-free exosomes generated from hMSCs cultured in 2-dimensional (2D) conventional conditions or in 3-dimensional (3D) collagen scaffolds promote functional recovery and neurovascular remodeling in rats after TBI. Wistar rats were subjected to TBI induced by controlled cortical impact; 24 hours later tail vein injection of exosomes derived from hMSCs cultured under 2D or 3D conditions or an equal number of liposomes as a treatment control were performed. The modified Morris water maze, neurological severity score and footfault tests were employed to evaluate cognitive and sensorimotor functional recovery. Animals were sacrificed at 35 days after TBI. Histological and immunohistochemical analyses were performed for measurements of lesion volume, neurovascular remodeling (angiogenesis and neurogenesis), and neuroinflammation. Compared with liposome-treated control, exosome-treatments did not reduce lesion size but significantly improved spatial learning at 33-35 days measured by the Morris water maze test, and sensorimotor functional recovery, i.e., reduced neurological deficits and footfault frequency, observed at 14-35 days post injury ($p < 0.05$). Exosome treatments significantly increased the number of newborn endothelial cells in the lesion boundary zone and dentate gyrus, and significantly increased the number of newborn mature neurons in the dentate gyrus as well as reduced neuroinflammation. Exosomes derived from hMSCs cultured in 3D scaffolds provided better outcome in spatial learning than exosomes from hMSCs cultured in the 2D condition. In conclusion, hMSC-generated exosomes significantly

Address correspondence to: Ye Xiong, MD, PhD, Department of Neurosurgery, Henry Ford Health System, E&R Building, Room # 3096, 2799 West Grand Boulevard, Detroit, MI 48202, Tel: 313-916-4743, Fax: 313-916-9855, yxiong1@hfhs.org.

Disclosure

We have filed a Disclosure to HFH, based on our work done in HFH with exosomes and scaffolds (MC, ZGZ, YX).

improve functional recovery in rats after TBI, at least in part, by promoting endogenous angiogenesis and neurogenesis and reducing neuroinflammation. Thus, exosomes derived from hMSCs may be a novel cell-free therapy for TBI, and hMSC-scaffold generated exosomes may selectively enhance spatial learning.

Keywords

exosomes; function recovery; human mesenchymal stem cell (hMSC); neuroinflammation; scaffolds; traumatic brain injury

Introduction

Traumatic brain injury (TBI) is a major cause of death and long-term disability worldwide (Marklund and Hillered, 2011). Effective pharmacologic treatments have not been identified from clinical trials in TBI (Narayan et al., 2002; Skolnick et al., 2014; Wright et al., 2014; Xiong et al., 2013). There is a compelling need to develop therapeutic approaches designed to improve functional recovery after TBI. Multipotent mesenchymal stem cells (MSCs) are a heterogeneous subpopulation consisting of mesenchymal stem and progenitor cells that can be harvested from bone marrow, umbilical cord blood, peripheral blood, adipose tissue and skin, as well as other organs (Ho et al., 2008; Walker et al., 2009). MSCs have shown promise as an effective therapy for brain injuries in experimental models of TBI and stroke (Chen et al., 2001a; Chen et al., 2003; Chopp and Li, 2002; Li et al., 2002; Li and Chopp, 2009; Lu et al., 2001b; Mahmood et al., 2004a, b; Nichols et al., 2013) and potentially in clinical settings (Cox et al., 2011; Doeppner and Hermann, 2014; Zhang et al., 2008). MSC-seeded collagen scaffolds that provide a three-dimensional (3D) environment to mimic the natural extracellular matrix have demonstrated therapeutic potential in preclinical studies of TBI (Lu et al., 2007; Mahmood et al., 2011; Mahmood et al., 2014a; Mahmood et al., 2014b; Qu et al., 2011; Qu et al., 2009; Xiong et al., 2009). Previous studies show that only a small proportion of transplanted MSCs actually survive and few MSCs differentiate into neural cells in injured brain tissues (Li et al., 2001; Lu et al., 2001b). The predominant mechanisms by which MSCs participate in brain remodeling and functional recovery are likely related to their secretion-based paracrine effect rather than a cell replacement effect (Chopp and Li, 2002; Li and Chopp, 2009). Our previous in vitro data show that collagen scaffolds stimulate human MSCs (hMSCs) to express multiple factors related to angiogenesis and neurogenesis, and signal transduction, which may contribute to hMSC survival, tissue repair, and functional recovery after TBI (Qu et al., 2011). Treatment of TBI with 3D collagen scaffolds impregnated with hMSCs significantly decreases functional deficits, promotes neurovascular remodeling, suppresses expression of axonal growth inhibitory molecules (for example, neurocan and Nogo-A) compared to the hMSCs group (Mahmood et al., 2011; Mahmood et al., 2014a; Mahmood et al., 2014b; Qu et al., 2011; Xiong et al., 2009).

Exosomes are endosomal origin small-membrane vesicles with a size of approximately 30 to 120 nm in diameter (Simons and Raposo, 2009; Vlassov et al., 2012). They are released by almost all cell types and contain not only proteins and lipids, but also messenger RNAs and

micro RNAs (miRNAs) (Barteneva et al., 2013). Increasing evidence indicates that exosomes have a pivotal role in cell-to-cell communication (Pant et al., 2012). In contrast to transplanted exogenous MSCs, nanosized exosomes derived from MSCs do not proliferate, are less immunogenic and easier to store and deliver than MSCs (Lai et al., 2011). Recent studies indicate that exosomes and microvesicles derived from multipotent MSCs have therapeutic promise in cardiovascular, kidney, liver and lung diseases (Akyurekli et al., 2015; Borges et al., 2013; Cosme et al., 2013; Lai et al., 2011; Lai et al., 2015; Liang et al., 2014; Masyuk et al., 2013; Yu et al., 2014). We have demonstrated that exosomes generated from rat MSCs improve functional recovery in rats after stroke (Xin et al., 2013b) and TBI (Zhang et al., 2015). A recent study indicated that extracellular vesicles isolated from human MSCs rescued pattern separation and spatial learning impairments in mice one month after TBI (Kim et al., 2016). However, whether exosomes generated from hMSCs promote neurovascular remodeling and functional recovery after TBI and whether exosomes derived from hMSCs cultured under 2-dimensional (2D) or 3D conditions have any differential therapeutic effect, have not been investigated. In the present study, we investigated the effects of exosomes generated from hMSCs cultured in 2D conventional condition or in 3D collagen scaffolds on cognitive and sensorimotor functional recovery as well as the potential mechanisms underlying therapeutic effects in rats after TBI.

Materials and Methods

All experimental procedures were approved by the Henry Ford Health System Institutional Animal Care and Use Committee. To prevent potential biases of performance and detection, the persons who performed the experiments, collected data, and assessed outcome were blinded throughout the course of the experiments and were unaware of the treatment allocation.

Preparation of hMSCs and exosomes

hMSCs were provided by Theradigm (Bethesda, MD) and expanded, as previously described (Digirolamo et al., 1999; Qu et al., 2009). In brief, hMSCs at passage 5 were plated at a concentration of 3×10^6 cells/75 cm^2 in tissue culture flasks with 20 ml low-glucose Dulbecco's modified Eagle's medium (Gibco BRL, Grand Island, NY) and were supplemented with 20% fetal bovine serum (Gibco BRL), 100 U/ml penicillin, 100 mg/ml streptomycin, and 2 mmol/L l-glutamine. For the exosome isolation, conventional culture medium was replaced with an exosome-depleted fetal bovine serum-contained (EXO-FBS-250 A-1, System Biosciences, Mountain View, CA, USA) medium when the cells reached 60% to 80% confluence, and the hMSCs were cultured for an additional 48 hours. The media were then collected and exosomes were isolated by ExoQuick exosome isolation method according to the manufacture's instruction. In brief, ExoQuick-TC (2.5 ml) was added to 10 ml of media, incubated 12 hours at 4°C, and centrifuged at 1500 × g for 30 min to obtain pelleted exosomes. The supernatant (non-exosomal fraction) of the samples were removed without disturbing the exosome pellets, and exosome pellets were resuspended in 200 μl of PBS. We quantitated the exosomes by measuring the total protein concentration using the micro Bicinchoninic Acid protocol (Pierce, Rockford, IL, USA) and analyzed

particle size and number using a qNano nanopore-based exosome detection system according to the manufacturer's instructions (Izon, Christchurch, New Zealand).

Scaffold Preparation, Cell Seeding and Exosome Collection

Ultrafoam scaffolds, collagen type I, were obtained from commercial sources (Avitene Ultrafoam collagen hemostat, cat # 1050030, Davol, Cranston, RI). The samples were cut into 5 mm discs (~ 5 mm thick) under sterile conditions from the larger collagen sheets. Avitene Ultrafoam is an absorbable hemostatic sponge prepared as a sterile, porous, pliable, water insoluble partial hydrochloric acid salt of purified bovine corium collagen. The scaffolds were pre-wetted overnight at 4°C (approximately 12 h) in culture medium consisting of DMEM supplemented with 10% fetal calf serum, 100 U/mL penicillin, 100 μg/mL streptomycin, 0.1 mM non-essential amino acids, and 1 ng/mL of basic fibroblast growth factor (Life Technologies, Rockville, MD). The scaffolds were then aseptically transferred using tweezers (1 scaffold per tube) to 50-mL sterile centrifuge tubes, allowing the scaffolds to sit at the bottom of the tubes. Seeding of hMSCs on scaffolds was performed, as previously described (Lu et al., 2007).

Following trypsinization of hMSCs from *ex vivo* expansion conditions, hMSCs at passage 5 were resuspended thoroughly and transferred gently (3×10^6 hMSCs per scaffold) into 200 μl of culture medium. Culture medium (100 μl) was then applied two times successively to opposite sides of the body of the cylindrical scaffold. The scaffold and cell solution were incubated for 30 min in a humidified incubator to facilitate primary cell seeding. The scaffolds were agitated gently within the solution manually twice every 15 min during this time. Following primary seeding, the centrifuge tubes were filled with an additional 3 mL of culture medium and placed in a humidified incubator overnight (Xiong et al., 2009). For the exosome isolation, conventional culture medium was replaced with an exosome-depleted FBS-contained medium when the cells reached 60% to 80% confluence, and the hMSCs were cultured for an additional 48 hours. The media were then collected and exosomes were isolated by ExoQuick exosome isolation method according to the manufacture's instruction, as described above.

Thirty μg of exosomal proteins was separated by SDS-PAGE using 8% high-bis polyacrylamide gels. The bands were then digested overnight. The peptides were separated by reversed-phase chromatography (Acclaim PepMap100 C18 column, Thermo Scientific), followed by ionization with the Nanospray Flex Ion Source (Thermo Scientific), and introduced into a Q Exactive mass spectrometer (Thermo Scientific). Abundant species were fragmented with high energy collision-induced dissociation (HCID). Data analysis was performed using Proteome Discoverer 2.1 (Thermo Scientific) which incorporated the Sequest (Thermo Scientific) algorithm.

Liposome Preparation

Liposomes are synthetic versions of natural vesicles such as exosomes. In order to mimic the exosomal lipid layer, we have prepared liposome based on three major fatty acids that are found in exosomal lipid analysis. Liposomes were prepared via the thin-film hydration technique (Ekanger et al., 2014). Briefly, to a 4 mL vial was added 1,2-dipalmitoyl-*sn*-

glycero-3-phosphocholine (14.0 mg, 19 μmol), 1,2-distearoyl-*sn*-glycero-3-phosphocholine (4.0 mg, 5 μmol), 1,2-dioleoyl-*sn*-glycero-3-phosphocholine (4.0 mg, 5 μmol), cholesterol (8.0 mg, 2.1 μmol), and chloroform (1 mL) to produce a clear, colorless solution. Solvent was removed under reduced pressure to afford a visible film on the bottom of the vial. The hydration solution, PBS (1.15 mL) and vial containing the lipid thin film were placed in a water bath at 60 °C for 30 min, and then the hydration solution was added to the vial containing the thin film. The resulting white suspension was stirred at 60 °C for 1 h. Extrusion of the suspension was accomplished using a mini-extruder and heating block (Avanti Polar Lipids, Alabaster, AL, USA) heated to 60 °C (4 passes through a 0.2 μm polycarbonate filter followed by 15 passes through a 0.1 μm polycarbonate filter). After extrusion, the suspension was allowed to cool to ambient temperature. Liposome samples were prepared for light scattering experiments by diluting liposome suspensions in phosphate-buffered saline (PBS, 1:10, 29 mM Na2HPO4, 46 mM NaH2PO4, 57 mM NaCl, and 2.1 mM KCl). Dynamic light scattering (DLS) data were obtained using a Malvern Zetasizer Nano-ZS instrument (ZEN3600) operating with a 633 nm wavelength laser. Dust was removed from samples by filtering through 0.2 μm hydrophilic filters (Millex–LG, SLLGR04NL). The size distribution of the prepared liposome was determined by DLS and the effective diameter was about 134 nm which is in agreement with the previous report of exosomal size (Villarroya-Beltri et al., 2013).

Animal Model and Experimental Groups

A well-established controlled cortical impact (CCI) rat model of TBI was utilized for the present study (Dixon et al., 1991). Adult male Wistar rats weighing 317 ± 10 g (2-3 months old) were anesthetized with chloral hydrate (350 mg/kg body weight, intraperitoneally). Rectal temperature was maintained at 37 ± 5°C using a feedback-regulated water-heating pad. Rats were placed in a stereotactic frame. Two 10-mm-diameter craniotomies were performed adjacent to the central suture, midway between Lambda and Bregma. The second craniotomy allowed for lateral movement of cortical tissue. The dura mater was kept intact over the cortex. Cortical injury was delivered by impacting the left cortex (ipsilateral cortex) with a pneumatic piston containing a 6-mm-diameter tip at a rate of 4 m/s and 2.5 mm of compression. Velocity was measured with a linear velocity displacement transducer.

The study animals were randomly divided into the following groups (n = 8/group): 1) Sham (craniotomies without injury and treatment), 2) TBI + liposomes (Lipo), 3) TBI + exosomes from hMSCs in 2D culture (Exo-2D), 4) TBI+ exosomes from hMSCs in 3D culture (Exo-3D). Exosomes generated from hMSCs in 2D or 3D conditions (100 μg total protein of exosome precipitate in 0.5 ml PBS/rat, ~=3×10^9 particles) or an equal volume of PBS containing 3×10^9 liposomes (0.5 ml) was administered intravenously over 5 min via tail vein, starting 1 day after injury. The dose of exosomes was chosen based on our previous studies with exosomes in rats after stroke (Xin et al., 2013b) and TBI (Zhang et al., 2015). TBI animals treated with liposomes were used as a control group. Liposomes (the liposome mimic of exosome lipid contents) we administered have the same lipid components as exosomes but lack content of proteins and genetic materials. We generated liposomes mimicking the primary content of the exosome lipid/phospholipid content. We performed the control treatment with the artificial exosome membrane consisting of the same lipid

content as exosomes to tease out potential therapeutic effects of exosomes in part due to their structural components. Sham animals underwent surgery without injury and treatment. For labeling proliferating cells, 5-bromo-2'-deoxyuridine (BrdU, 100 mg/kg) was injected intraperitoneally into rats daily for 10 days, starting 1 day after TBI. The dose and time for BrdU injection was based on our previous TBI studies in rats (Xiong et al., 2011a). All animals were allowed to survive 35 days after TBI.

Evaluation of Neurological Outcome

Modified Neurological Severity Score (mNSS) Test—Neurological functional measurement was performed using the mNSS test (Chen et al., 2001b). The test was carried out on all rats prior to injury and at 1, 4, 7, 14, 21, 28 and 35 days after TBI. The mNSS is a composite of the motor (muscle status, abnormal movement), sensory (visual, tactile, and proprioceptive), and reflex tests and has been used in previous studies (Lu et al., 2007; Mahmood et al., 2014b). Neurological function was graded on a scale of 0 to 18 (normal score 0; maximal deficit score 18). In the severity scores of injury, one point is awarded for each abnormal behavior or for lack of a tested reflex; thus, the higher the score, the more severe the injury.

Footfault Test—To evaluate sensorimotor function, the footfault test was carried out before TBI and at 1, 4, 7, 14, 21, 28 and 35 days after TBI. The rats were allowed to walk on a grid. With each weight-bearing step, a paw might fall or slip between the wires and, if this occurred, it was recorded as a foot fault (Baskin et al., 2003). A total of 50 steps were recorded for the right forelimb.

Morris Water Maze (MWM) Test—To measure spatial learning impairments, an updated version of the MWM test was used (Choi et al., 2006). The procedure was modified from previous versions (Morris et al., 1982), and has been used for spatial memory assessment in rodents with brain injury (Choi et al., 2006). The MWM test was performed monthly post-injury. At each testing interval, animals were tested with 4 trials per day for 5 consecutive days on Day 31-35 after TBI. A blue swimming pool (1.8 m in diameter) was located in a large room, where there were many clues external to the maze (e.g., pictures on the walls, lamps and a camera on the ceiling); these were visible from the pool and presumably used by the rats for spatial orientation. The position of the cues remained unchanged throughout the experiment. Data collection was automated using the Human Visual Image (HVS) Image 2020 Plus Tracking System (US HVS Image, San Diego, CA), as described previously (Mahmood et al., 2007). For data collection, the swimming pool was subdivided into four equal quadrants formed by imaging lines. At the start of each trial, the rat was placed at one of four fixed starting points, randomly facing toward a wall (designated North, South, East and West) and allowed to swim for 90 seconds or until it found the platform which was transparent and invisible to animals. If the animal found the platform by spatial navigation, it was allowed to remain on it for 10 seconds. Throughout the test period, the platform was located in the northeast (NE) quadrant 2 cm below water in a randomly changing position, including locations against the wall, toward the middle of the pool, or off-center but always within the target quadrant. If the animal was unable to locate the platform within 90 seconds, the trial was terminated after being guided onto the platform and remaining on it for 10

seconds, and a maximum score of 90 seconds was assigned. The percentage of time the animals spent swimming within the target quadrant relative to the total amount of time swimming in the maze before reaching the hidden platform or within 90 seconds for those rats that failed to find the platform was recorded for statistical analysis. The latency to find the hidden escape platform was also recorded and analyzed. In the traditional version of the MWM test, the position of the hidden platform is always fixed and is relatively easy for rodents. With the modified MWM test we used in this study, the platform is relocated randomly within the correct quadrant with each training trial. The rodents must spend more time searching within the target quadrant; therefore each trial effectively acts as a probe trial. The advantage of this protocol is that rodents should find the platform purely and extensively by reference to the extra-maze spatial cues, which improves the accuracy of spatial performance in the MWM (Choi et al., 2006).

Tissue Preparation

Rats were anesthetized with chloral hydrate administered intraperitoneally and perfused transcardially with saline solution, followed by 4% paraformaldehyde in 0.1 M PBS, pH 7.4. Rat brains were removed and immersed in 4% paraformaldehyde for 2-4 days. Using a rat brain matrix (Activational Systems Inc.), each forebrain was cut into 2- mm thick coronal blocks for a total 7 blocks from Bregma 5.2 mm to Bregma −8.8 mm per animal (Paxinos and Watson, 1986). The tissues were embedded in paraffin and a series of 6 μm-thick slides were cut. For lesion volume measurement, one 6-μm-thick section from each of 7 coronal blocks was traced by a microcomputer imaging device (MCID) (Imaging Research, St. Catharine's, Ontario, Canada), as described previously (Chen et al., 2005). The volumes of the ipsilateral and contralateral cortices were computed by integrating the area of each cortex measured at each coronal level and the distance between two sections. The cortical lesion volume was expressed as a percentage calculated by [(contralateral cortical volume – ipsilateral cortical volume)/(contralateral cortical volume) × 100% (Swanson et al., 1990).

Immunohistochemistry

Antigen retrieval was performed by boiling brain sections in 10 mM citrate buffer (pH 6.0) for 10 minutes. After washing with PBS, sections were incubated with 0.3 % H_2O_2 in PBS for 10 minutes, blocked with 1% BSA containing 0.3 % Triton-X 100 at room temperature for 1 hour, and incubated with anti-endothelial barrier antigen (EBA, 1:1000; COVANCE, CA) or anti-CD68 (1:200; Serotec, Kidlington, UK) or anti-glial fibrillary acidic protein (GFAP, 1:1000; Dako, Denmark) at 4°C overnight. For negative controls, primary antibodies were omitted. After washing, sections were incubated with biotinylated anti-mouse or anti-rabbit antibodies (1:200; Vector Laboratories, Inc.) at room temperature for 30 minutes. After an additional washing, sections were incubated with an avidin-biotin-peroxidase system (ABC kit, Vector Laboratories, Inc.), visualized with diaminobenzidine (Sigma), and counterstained with hematoxylin.

Immunofluorescent Staining

Newly generated endothelial cells and newborn mature neurons in the lesion boundary zone and dentate gyrus 35 days after TBI were identified by double labeling for BrdU with EBA or neuronal nuclei (NeuN), respectively. In brief, after being deparaffinized and rehydrated,

brain sections were boiled in 10 mM citric acid buffer (pH 6) for 10 minutes. After washing with PBS, sections were incubated in 2.4 N HCl at 37°C for 20 minutes. Sections were incubated with 1% BSA containing 0.3% Triton-X-100 in PBS. Sections were then incubated with mouse anti-NeuN antibody (1:200; Chemicon, Temecula, CA) or anti-EBA at 4°C overnight. For negative controls, primary antibodies were omitted. FITC-conjugated anti-mouse antibody (1:400; Jackson ImmunoResearch, West Grove, PA) was added to sections at room temperature for 2 hours. Sections were then incubated with rat anti-BrdU antibody (1:200; Dako, Glostrup, Denmark) at 4°C overnight. Sections were then incubated with Cy3-conjugated goat anti-rat antibody (1:400; Jackson ImmunoResearch, West Grove, PA) at room temperature for 2 hours. Each of the steps was followed by three 5-minute rinses in PBS. Tissue sections were mounted with Vectashield mounting medium (Vector laboratories, Burlingame, CA).

Cell Counting and Quantitation

A series of 6-μm-thick coronal sections were cut through the dorsal hippocampus containing the DG between Bregma −3.0 to −4.5 for all rats. Every 6th coronal section for a total of five sections with 30-μm intervals was used for immunohistochemical staining and analyzed with a microscope (Nikon i80) at 400× magnification via the MCID system. CD68+ microglia/macrophages, EBA+ endothelial cells, GFAP+ astrocytes, BrdU+ cells, and EBA/BrdU-colabeled cells were counted in the lesion boundary zone and the dentate gyrus (DG). For analysis of neurogenesis, we counted NeuN/BrdU-colabeled cells in the DG and its subregions, including the subgranular zone, granular cell layer, and the molecular layer. The fields of interest were digitized under the light microscope (Nikon, Eclipse 80i) at a magnification of either 200 or 400 using CoolSNAP color camera (Photometrics) interfaced with MetaMorph image analysis system (Molecular Devices), as described in detail previously (Zhang et al., 2013b). In brief, five fields of view in the lesion boundary zone from the epicenter of the injury cavity (Bregma −3.3 mm), and 9 fields of view in the ipsilateral DG were counted in the each section. From our previous experience, our inter-rater reliability was greater than 95% when the cell counts were compared between two independent trained blinded observers scoring the same sections of an animal. All counting was performed on a computer monitor to improve visualization and in one focal plane to avoid oversampling (Xiong et al., 2011a; Zhang et al., 2002). BrdU and NeuN double immunofluorescently reactive cells were further assessed using a Zeiss LSM 510 META confocal microscope. In the present study, one blinded observer performed the cell counting in all brain sections.

Statistical Analysis

Data are presented as the means with standard deviations. The analysis of variance (ANOVA) was used for repeated measurements of spatial performance and sensorimotor function. For cell counting, a one-way ANOVA followed by post hoc Tukey’s tests was used to compare the differences between the exosome-treated, liposome-treated and sham groups. Pearson's correlation coefficients were calculated to examine relationships between cognitive functional recovery and immunostaining. Differences were considered significant if the P value was <0.05.

Results

Isolation of Exosomes from hMSCs Cultured in 2D and 3D Conditions

In the present study, we employed the ExoQuick-TC kit with centrifugation to isolate exosomes (Taylor et al., 2011). Due to the relatively low centrifugal force employed in the ExoQuick isolation process, the precipitation of non-exosomal proteins and nucleotides is minimized, whereas non-exosomal protein contamination can occur in prolonged ultra-centrifugation methods (Cvjetkovic et al., 2014). The protein amount of exosomes generated from 3×10^6 hMSCs in the 3D condition was 2 times higher than that of those in the 2D condition (168.5 ± 11.2 μg for 3D vs 84.7 ± 5.5 μg for 2D, $p<0.05$). Exosomes were isolated from culture media where 3×10^6 hMSCs were cultured in 2D dish or 3D scaffold in the exosome-depleted FBS-contained medium for 2 days. We also performed proteomic analysis on the exosomes. Multiple exosomal CD marker proteins were detected in the exosomes, including CD9, CD63, and CD81 in both 2D and 3D cultures. These data strongly support that these nanoparticles are exosomes.

hMSC Exosome Administration Does Not Alter Cortical Lesion Volume in Rats after TBI

Cortical lesion volume was measured 35 days post TBI, as described previously (Xiong et al., 2011b). No differences in the lesion volume were observed between the liposome group and exosome groups (16.4 ± 0.2% for Lipo group, 16.2 ± 0.4% for Exo-2D group,

16.0 ± 0.3% for Exo-3D group, **Fig.1**, $p > 0.05$).

hMSC Exosome Administration Significantly Promotes Sensorimotor Functional Recovery in Rats after TBI

Neurological functional measurement was performed on rats using the mNSS test. The higher the score, the more severe the injury. The mNSS score was close to 12 in TBI rats (both the Lipo and exosome groups) on Day 1 post TBI, indicating neurological functional deficits were comparable in all TBI rats before treatment (**Fig. 2A**, $p > 0.05$). Significant reduction in the mNSS score was found over time in the liposome-treated animals starting from Day 4-35 compared to Day 1 post injury ($p < 0.05$), suggesting a significant spontaneous sensorimotor functional recovery occurred after TBI. However, compared to the liposome treatment, functional recovery was significantly improved in the exosome-treated groups on Days 14-35 after TBI (at Day 14-35, $p < 0.05$, with ANOVA followed by post-hoc Tukey's tests). Exosome treatment also significantly reduced the frequency of forelimb footfault occurrence as compared to liposome controls (**Fig. 2B**, at Day 14-35, $p < 0.05$, with ANOVA followed by post-hoc Tukey's tests). Although both Exo-2D and Exo-3D treatments significantly improved sensorimotor functional recovery compared to the liposome treatment, there is no significant difference in mNSS score and footfault test between the Exo-2D and Exo-3D groups.

hMSC Exosome Administration Significantly Enhances Spatial Learning in Rats after TBI

Spatial learning measurements were performed during the last five days (31-35 days post injury) prior to sacrifice using a modified MWM test, which is very sensitive to the hippocampal injury (Choi et al., 2006). The greater the percentage of time the animals spend

in the correct quadrant (i.e., Northeast, where the hidden platform was located) in the water maze, the better the spatial learning function. The percentage of time spent by sham rats in the correct quadrant increased significantly from 32-35 days after sham operation, compared to time spent in the correct quadrant at the first day of testing, that is, Day 31 (**Fig. 3A**, $p < 0.05$). In the testing of spatial memory among 3 groups, no significant between-group effect on the time spent in the correct quadrant was detected on the first day of the testing in the MWM test (Day 31 post injury, $p > 0.05$); however, a statistically significant between-group effect on the time spent in the correct quadrant was noted in the MWM test (at Day 33-35, $p < 0.05$). Relative to the liposome group, post-hoc Tukey's testing demonstrated significantly increased time spent in the correct quadrant in the exosome groups at Day 33-35 with significantly improved benefits from Exo-3D treatment compared with the Exo-2D treatment ($p < 0.05$).

Another important parameter for assessing spatial learning in the MWM test is the time (referred as latency) for animals to find the hidden platform in the correct quadrant (Zhang et al., 2013b). The less time for animals to find the platform, the better the spatial learning function. During the first day of testing (that is, 31 days post injury), no significant between-group effect on the time for animals to find the hidden platform in the correct quadrant was detected in the MWM test (**Fig. 3B**, $p = 0.338$); however, sham animals took significantly less time to find the hidden platform in the correct quadrant compared to other groups during the second day of testing (at Day 32, $p < 0.05$). Relative to the liposome group, post-hoc Tukey's testing demonstrated significantly less time for animals to find the platform in the exosome groups during the last 3 day testing, that is, at Day 33-35 ($p < 0.05$). Relative to the Exo-2D group, animals in the Exo-3D group took significantly less time to find the hidden platform at Day 33-35 ($p < 0.05$).

Our data demonstrated that there were no significant difference in the swim speeds between groups (**Fig. 3C,** $p > 0.05$), indicating that land-based motor deficits did not affect swimming speed and therefore impaired spatial learning and memory did not result from effect of motor deficits. Swim path lengths for the liposome-treated TBI rats were significantly greater than those for Sham rats and Exo-2D and Exo-3D-treated TBI rats (**Fig. 3D**, $p<0.05$), suggesting that TBI rats treated with liposomes exhibited impaired spatial memory compared with Exo-2D and Exo-3D-treated TBI rats.

hMSC Exosome Administration Significantly Increases Vascular Density and Angiogenesis in Rats after TBI

EBA-staining was performed to identify mature vasculature in the brain after TBI (Li et al., 2007). TBI alone significantly increased the density of vessels in the lesion boundary zone and DG of the ipsilateral hemisphere compared to sham controls (**Fig. 4**, $p < 0.05$). Exosome treatments significantly increased the vascular density in the injured cortex and DG compared to the liposome treatment (**Fig. 4**, $p < 0.05$, with ANOVA followed by post-hoc Tukey's tests). Exosome treatment significantly increased angiogenesis identified by EBA/BrdU+ double labeling for newborn endothelial cells in the lesion boundary zone and DG compared to the liposome treatment (**Fig. 4,** $p < 0.05$). The Pearson's correlation analyses further showed that: 1) spatial learning was positively correlated to EBA+ vascular density

in the DG region ($R^2 = 0.87$, $p < 0.05$); and 2) sensorimotor functional recovery was positively correlated to EBA+ vascular density in the lesion boundary zone ($R^2 = 0.75$, $p < 0.05$). Although both Exo-2D and Exo-3D treatments significantly promoted angiogenesis compared to the liposome treatment, there is no significant difference between the Exo-2D and Exo-3D groups.

hMSC Exosome Administration Significantly Increases Neurogenesis in the DG in Rats after TBI

To investigate cell proliferation in the DG, we injected BrdU ip into rats once daily for 10 days starting 24 hours post injury. Animals were sacrificed at 35 days after TBI, and immunostaining were performed on paraffin-embedded brain coronal sections (Meng et al., 2011). TBI alone significantly increased cell proliferation compared to Sham group. Exosome therapy did not significantly increase the number of BrdU-positive cells compared to the liposome treatment (**Fig. 5A-D**, $p < 0.05$). To identify newly generated neurons in the DG, double staining for BrdU (proliferating marker, **Fig. 5E-H**) and NeuN (mature neuronal marker, **Fig. 5I-L**) was performed. BrdU and NeuN double immunofluorescently reactive cells were further assessed using a Zeiss LSM 510 META confocal microscope (**Fig. 5M**). Exosome treatment significantly increased the number of newborn neurons detected in the granule layer of the DG compared to the liposome controls (**Fig. 5N-O**, $p < 0.05$). Relative to the Exo-2D treatment, the Exo-3D treatment significantly increased the number of newborn mature neurons detected in the DG ($p < 0.05$). Our data show a significant positive correlation between spatial learning tested by the MWM test and the number of newborn mature neurons in the DG ($R^2 = 0.73$, $p<0.05$).

hMSC Exosome Administration Significantly Reduces Brain Inflammation in Rats after TBI

GFAP-staining was performed to identify reactive astrocytes in the brain after TBI (Schwab et al., 2001). TBI alone significantly increased the number of GFAP+ cells in the lesion boundary zone and DG of the ipsilateral hemisphere compared to sham controls (**Fig. 6**, $p < 0.05$). Exosome treatment significantly reduced the GFAP+ astrocyte density in the injured cortex and DG compared to the liposome treatment (**Fig. 6**, $p < 0.05$, with ANOVA followed by post-hoc Tukey's tests). The Pearson's correlation analyses showed that: 1) spatial learning was inversely correlated to GFAP+ astrocyte density in the DG region ($R^2 = 0.86$, $p < 0.05$); and 2) sensorimotor functional recovery was inversely correlated to GFAP+ astrocyte density in the lesion boundary zone ($R^2 = 0.77$, $p < 0.05$). CD68-staining was performed to identify activated macrophages/microglia in the brain after TBI (Li et al., 2009). TBI alone significantly increased the number of CD68+ cells in the lesion boundary zone and DG of the ipsilateral hemisphere compared to sham controls (**Fig. 6**, $p < 0.05$). Exosome treatments significantly reduced the CD68+ cell number in the injured cortex and DG compared to the liposome treatment (**Fig. 6**, $p < 0.05$, with ANOVA followed by post-hoc Tukey's tests). Relative to the Exo-2D treatment, the Exo-3D treatment significantly decreased the number of CD68+ cells detected in the DG ($p < 0.05$). The Pearson's correlation analyses showed that: 1) spatial learning was inversely correlated to CD68+ cell density in the DG region ($R^2 = 0.75$, $p < 0.05$); and 2) sensorimotor functional recovery was inversely correlated to CD68+ cell density in the lesion boundary zone ($R^2 = 0.55$, $p < 0.05$).

Discussion

In the present study, we demonstrate for the first time that systemic administration of cell-free exosomes generated by hMSCs cultured under 2D and 3D conditions, with treatment initiated 24 hours post injury in a rat model of TBI does not alter cortical lesion volume compared to the liposome treatment control, but significantly: 1) improves cognitive and sensorimotor functional recovery; 2) increases the number of newborn mature neurons in the DG; and 3) increases the number of newborn endothelial cells in the lesion boundary zone and DG; 4) reduces neuroinflammation; and 5) exosomes generated from hMSCs cultured in 3D condition provide better outcome in spatial learning compared to exosomes from 2D culture. Exosome treatments initiated 24 h post injury did not reduce lesion volume, suggesting that beneficial effects of exosomes is not attributed to direct neuroprotection, but, rather to neurovascular remodeling. Improved functional recovery after treatment of TBI with exosomes generated from hMSCs is significantly associated with increased brain angiogenesis and neurogenesis as well as with reduced neuroinflammation. Our results suggest that intravenous administration of exosomes generated from hMSCs may represent a novel cell-free therapeutic approach for treatment of TBI.

MSCs alone and MSCs seeded into scaffolds improve functional outcome in animal models of stroke and TBI (Kim et al., 2010; Lu et al., 2007; Mahmood et al., 2004a; Mahmood et al., 2005, 2007; Mahmood et al., 2014a; Mahmood et al., 2014b; Peng et al., 2015; Qu et al., 2011; Qu et al., 2008; Xiong et al., 2009). The mechanisms underlying improvement in MSC-induced functional recovery after TBI are not clear. Our recent study shows that intravenous administration of cell-free MSC-generated exosomes improves functional recovery and enhances neurite remodeling, neurogenesis, and angiogenesis in rats after stroke (Xin et al., 2013b). The beneficial effects of systemic administration of MSCs and cell-free exosomes generated by MSCs appear similar in animal models of stroke and TBI (Chopp and Li, 2002; Li et al., 2012; Xin et al., 2013b), in terms of improved functional recovery and increased neuroplasticity including angiogenesis and neurogenesis. These data support the hypothesis that beneficial effects of MSC treatment are at least partly mediated by exosomes from hMSCs. Cells produce exosomes with components and functions that mirror those of their parent cells (Katsuda et al., 2013). Exosomes contain proteins, lipids, messenger RNAs and microRNAs, which can be transferred to recipient cells and modify their characteristics (Xu et al., 2013). Selective manipulation of specific molecules identified for a therapeutic effect in the parent MSCs may lead to an enhancement of the therapeutic efficiency of isolated exosomes, as demonstrated in our previous stroke study showing that exosomes from MSCs mediate the miR-133b transfer to astrocytes and neurons, which regulate gene expression, and subsequently increase neurite remodeling and functional recovery after stroke (Xin et al., 2013c). Further studies are warranted to identify the molecular constituents of the exosomes derived from hMSCs, including specific microRNAs and growth factors that promote angiogenesis and neurogenesis as well as reduce neuroinflammation after TBI.

In the present study, the 100 μg total protein of exosomes injected into each rat was collected from approximately 2×10^6 MSCs, a number of MSCs equivalent to the effective amount that we previously used in the MSC-based treatment for TBI (2×10^6 MSCs per rat) (Lu et

al., 2001b). Our present study demonstrated that hMSCs seeded in the 3D collagen scaffolds generated significantly more exosomes compared to the hMSCs in the 2D condition. This finding may partially explain why hMSCs seeded into scaffolds when transplanted to the injured brain provide better functional recovery after TBI compared to hMSCs alone, as shown in our previous studies (Lu et al., 2007; Mahmood et al., 2011). Whether a higher dose of exosomes provides a better functional recovery in rats after TBI requires investigation. Further studies are also warranted to determine specific contents of exosomes from hMSCs cultured in 3D condition as well as a dose-response efficacy for this novel mode of exosome treatment for TBI. In addition, we cannot exclude the possibility that exosomes may act, as possibly do cell-based therapies, on peripheral tissues to indirectly promote neurovascular remodeling and functional recovery post TBI. MSCs used as cell therapy after TBI may act as remote "bioreactors" via stimulation of lung macrophages and spleen T regulatory cell production (likely due to many intravenously injected MSCs trapped by these organs), leading to systemic remote effects on the central nervous system (Walker et al., 2012). It is warranted to investigate whether these nanosized exosomes are trapped in those organs and have remote effects on injured brain.

In a previous study, by tagging exosomes with green fluorescent protein (GFP), we demonstrated that exosomes-enriched particles generated from MSCs were taken up by astrocytes and neurons in the ischemic boundary zone in stroke rats after intravenous injection of MSCs (Xin et al., 2013c). Our previous study demonstrated that exosomes generated from MSCs in 2D culture effectively improve functional recovery by enhancing endogenous angiogenesis and neurogenesis and reducing neuroinflammation in TBI rats that received iv 100 μg of exosomes 24 h post injury (Zhang et al., 2015). In a recent study, Kim et al. reported that exosomes isolated from MSCs in 2D culture improves cognitive function and reduces inflammation in TBI mice that received iv 30 μg of exosomes 1 h post injury (Kim et al., 2016). In the current study, we further demonstrated that exosomes isolated from 3D culture are superior to those in 2D culture in terms of improving cognitive functional recovery. Exosomes contain very complex molecular cargo (Lai et al., 2013; Yu et al., 2014). The benefit and potential strength of exosome treatment, as with stem-cell therapy, is its ability to affect multiple targets. We have demonstrated in stroke rats, that treatment with MSCs transfers microRNAs via exosomes to recipient parenchymal cells (Xin et al., 2013c). MicroRNAs regulate a myriad of genes (Lakshmipathy and Hart, 2008). It is likely that the multitargeted approach, rather than the traditional, single molecular pathway approach, elicits the therapeutic potency of exosomes or cell-based therapy. Treatment with MSC-generated exosomes is an alternative approach for targeting the complex TBI.

Our data demonstrate that intravenous administration of exosomes derived from hMSCs cultured in 2D and 3D conditions promotes neurogenesis in the DG after TBI. Neurogenesis (a complex process by which new neurons are generated from neural stem/progenitor cells during development) occurs in mammals during adulthood, and is involved in the pathology of different neurological disorders (Taupin, 2006). Thus, neurogenesis is a potential target for treatment of neurological diseases. TBI stimulates neurogenesis in rodents and humans (Kernie and Parent, 2010; Richardson et al., 2007; Zheng et al., 2013). There is a strong link between certain types of memory functions and adult neurogenesis in the hippocampus. For example, blocking neurogenesis genetically (Blaiss et al., 2011) or pharmaceutically (Zhang

et al., 2012) impairs spatial learning and memory after TBI, while enhancing neurogenesis promotes learning and memory (Kleindienst et al., 2005; Lu et al., 2005; Sun et al., 2007). Adult neurogenesis in the mammalian brain occurs primarily in the DG of the hippocampus and in the subventricular zone (SVZ) surrounding the lateral ventricle (Altman and Das, 1965; Lois and Alvarez-Buylla, 1993). In normal conditions, neuroblasts in the SVZ migrate along the rostral migratory stream to the olfactory bulb and differentiate into olfactory interneurons (Doetsch and Alvarez-Buylla, 1996). Some of neuroblasts generated in the SVZ can migrate to the injured cortical area after TBI and may be involved in brain injury repair (Jin et al., 2003; Parent et al., 2002; Sundholm-Peters et al., 2005). To date, there is no evidence for migration of SGZ-derived cells beyond the hippocampus after brain injury. In the DG, the newly generated cells of the subgranular zone (SGZ) migrate laterally into the granule cell layer and exhibit properties of fully integrated mature dentate granule neurons (Kempermann and Gage, 2000; van Praag et al., 2002b). Importantly, the newly generated DG granule neurons form synapses and extend axons into their correct target area, the CA3 region (Hastings and Gould, 1999).

Our data indicate that hMSC-derived exosome treatment enhances generation of newly born vessels (angiogenesis), which may contribute to functional recovery after TBI, as demonstrated by us and others (Lu et al., 2004; Morgan et al., 2007; Xiong et al., 2010). EBA+ cells are endothelial cells which constitute the vessels (Lin et al., 2001). Exosome treatment-induced angiogenesis may contribute motor functional recovery by promoting neurite growth and synaptogenesis in the brain after stroke (Xin et al., 2013b) because angiogenesis is well coupled with neurogenesis in the DG (Arai et al., 2009; Lo, 2008; Ohab et al., 2006; Xiong et al., 2011c). These neurovascular coupling and remodeling may act, in concert, to improve learning and memory after brain injury.

In the present study, cell-free exosomes derived from hMSCs promote neurovascular remodeling and improve functional recovery after TBI, which supports our previous findings indicating that the efficacy of MSC transplantation in treating TBI in animal models is independent of cell replacement (Chopp et al., 2008; Joyce et al., 2010). We have previously employed different routes (intraarterial, intravenous, and intracerebral) to administer MSCs into rodents with TBI (Lu et al., 2001a; Mahmood et al., 2004a; Mahmood et al., 2002). Although they exhibit promising therapeutic effects (Lu et al., 2001a; Mahmood et al., 2008; Mahmood et al., 2004a; Mahmood et al., 2002), there are some disadvantages for each route. Relatively few MSCs can be injected intracranially; intraarterial injection of MSCs can cause brain ischemia; and intravenous injection results in body-wide distribution of MSCs (Lu et al., 2007). Although transplantation of scaffolds seeded with MSCs into lesion cavity promotes functional recovery after TBI (Lu et al., 2007; Mahmood et al., 2011; Mahmood et al., 2014b; Xiong et al., 2009), it requires cranial surgery. Considering the nanosize of exosomes and their many advantages, exosomes present a novel weapon for the treatment of TBI in terms of easy administration and the potential drug delivery vehicles across the BBB (Alvarez-Erviti et al., 2011; Braccioli et al., 2014). Although cell-free exosome-based therapy offers several advantages over MSCs including easier storage and reduced safety risks, it is warranted to determine the safety of exosomes in animals before initiating clinical trials. Of note, a clinical trial testing effect of cell-free cord blood derived MSC

microvesicles/exosomes on β-cell mass in Type I Diabetes Mellitus among others is ongoing (ClinicalTrials.gov, NCT02138331).

In the current study, activation of GFAP+ astrocytes and CD68+ microglia/macrophages was significantly suppressed by exosomes compared to the liposome treatment control. This anti-inflammatory effect is similar to that of MSC therapy in animal models of stroke (Tsai et al., 2014; Xin et al., 2013a) and TBI (Zhang et al., 2013a). Astrocytes and microglia are distributed throughout the brain, and one of their main functions is to monitor and sustain neuronal health (Woodcock and Morganti-Kossmann, 2013). Activated astrocytes and microglia release pro and anti-inflammatory cytokines, free radicals, anti-oxidants, and neurotrophic factors which contribute to neuronal death as well as enhance survival mechanisms during neurodegeneration (Singh et al., 2011) and after TBI (Li et al., 2009; Zhang et al., 2012). It remains under debate whether activated microglia/macrophages promote neuronal survival or exacerbate neuronal damage (Hailer, 2008). Recent experimental evidence indicates that microglia under certain circumstances can be beneficial and support the different steps in neurogenesis, progenitor proliferation, survival, migration, and differentiation (Ekdahl et al., 2009). In the present study, we demonstrate that suppression of activated microglia/macrophages by treatment with exosomes may, at least in part, contribute to increased angiogenesis and neurogenesis, and subsequent improvement in functional recovery after TBI. The improved functional outcome in spatial learning from TBI rats treated with Exo-3D may be attributed to further enhanced neurogenesis and reduced activation of microglia/astrocytes in the DG compared to the Exo-2D group.

In the present 35-day study, the exosome treatment significantly accelerated functional recovery (that is, reduced mNSS and footfault scores) after TBI compared to the liposome treatment. TBI produces behavioral deficits, with different recovery rates over time, dependent on injury type, severity/size, sex, age, and different tasks performed (Ding et al., 2013; Ning et al., 2011; Nishibe et al., 2010; Smith et al., 2007). Our previous long-term (3-month) studies indicate that TBI animals without interventions continue to slowly recover after the 35 day time point (Mahmood et al., 2008; Ning et al., 2011). It is important to determine whether the exosome treatment has a long-term permanent reduction in chronic deficits in the future study. The present study provides evidence that exosome, and particularly 3D scaffold generated exosomes are beneficial for treatment of TBI. However, further studies are needed to optimize the exosome production and quality control, to determine dosing, timing, toxicity, mechanisms of MSC exosome treatment.

Some additional limitations should be noted in the present study. Extracellular particles and soluble factors are important mechanisms underlying MSC therapy (Lai et al., 2013; Lavoie and Rosu-Myles, 2013; Liang et al., 2013; Yu et al., 2014). Extracellular particles include released small homogenous exosomes of endocytic origin and heterogeneous microvesicles by the outward budding and fission of the plasma membrane (Gyorgy et al., 2011; Lavoie and Rosu-Myles, 2013). Although the supernatant of the samples were carefully removed after centrifugation, we do not exclude the possibility of microvesicle components in the content of our injected precipitate, and we will not exclude a contribution of microvesicles to mediating TBI recovery. In addition, we generate exosomes from hMSCs. We do not exclude the possibility that exosomes generated from other cells, e.g., embryonic stem cells,

may be as effective as or superior to a treatment for TBI. Exosomes derived from hMSCs contain multiple factors which may contribute to functional recovery post-TBI. This beneficial effect of the scaffold, may not be limited to exosomes derived from hMSCs. Possibly, exosomes harvested from other cells when placed in a 3D collagen scaffold matrix, may also exhibit enhanced restorative benefit for the treatment of TBI. We do not know how exosomes induce neurovascular remodeling, that is, which specific molecules are involved in these processes. Exosomes, depending on their parental origin, contain a variety of proteins, lipids, noncoding RNAs, mRNA, and miRNA, collectively termed as “cargo” contents (Kalani et al., 2014). Contained among these constituents, miRNAs may play a key role in mediating biological function due to their prominent role in gene regulation, as we demonstrate that MSCs communicate with brain parenchymal cells and regulate neurite outgrowth by transfer of miR-133b to neural cells via exosomes (Xin et al., 2012; Xin et al., 2014; Xin et al., 2013c; Zhang and Chopp, 2015, 2016). In addition, we performed the control treatment with the artificial exosome membrane, which consists of the same lipid content as exosomes but lacks content of proteins and genetic materials. We demonstrate that it is the content of the exosome and not the lipid membrane of the exosome that mediates functional recovery. In addition, we used equal (100 μg total protein) exosomes isolated from hMSCs in 2D or 3D conditions. Therefore, the content of the exosomes is responsible for the differential therapeutic effects, with the 3D conditioned exosomes likely containing a different profile of proteins and genetic materials compared to 2D exosomes.

In conclusion, in the present study, we for the first time demonstrate that intravenous administration of exosomes generated from hMSCs in 2D or 3D cultures improves functional recovery and promotes neurovascular remodeling (angiogenesis and neurogenesis) and reduces neuroinflammation in rats after TBI. Our discovery into the role of exosomes leads to further understanding into how hMSCs improve functional recovery after TBI. Cell-free exosomes may represent a novel and safer therapeutic refinement of MSCs for treatment of TBI and other neurological diseases.

Supplementary Material

Refer to Web version on PubMed Central for supplementary material.

Acknowledgements

The authors wish to thank Elizabeth Pikula, Qinge Lu, Julie Landschoot-Ward, and Sutapa Santra for the technical assistance and Dr. Yi Zhang for assistance in confocal microscopy. We acknowledge the assistance of the Wayne State University Proteomics Core in proteomic analysis of exosomes. This work was partially supported by National Institutes of Health R01 NS081189 (Dr. Xin), R01 NS088656 (Dr. Chopp), and P41 EB002520 (for the collagen sponge support).

Abbreviations

2D	2 dimension
3D	3 dimension
FBS	fetal bovine serum

MSC	mesenchymal stromal cell
TBI	traumatic brain injury
DG	dentate gyrus
EBA	endothelial barrier antigen
NeuN	neuronal nuclei
GFAP	glial fibrillary acidic protein
BrdU	bromodeoxyuridine
MWM	Morris water maze
mNSS	modified neurological severity score
MCID	microcomputer imaging device
ANOVA	Analysis of variance

References

Akyurekli C, Le Y, Richardson RB, Fergusson D, Tay J, Allan DS. A systematic review of preclinical studies on the therapeutic potential of mesenchymal stromal cell-derived microvesicles. Stem Cell Rev. 2015; 11:150–160. [PubMed: 25091427]

Alvarez-Erviti L, Seow Y, Yin H, Betts C, Lakhal S, Wood MJ. Delivery of siRNA to the mouse brain by systemic injection of targeted exosomes. Nat Biotechnol. 2011; 29:341–345. [PubMed: 21423189]

Arai K, Jin G, Navaratna D, Lo EH. Brain angiogenesis in developmental and pathological processes: neurovascular injury and angiogenic recovery after stroke. FEBS J. 2009; 276:4644–4652. [PubMed: 19664070]

Barteneva NS, Maltsev N, Vorobjev IA. Microvesicles and intercellular communication in the context of parasitism. Front Cell Infect Microbiol. 2013; 3:49. [PubMed: 24032108]

Baskin YK, Dietrich WD, Green EJ. Two effective behavioral tasks for evaluating sensorimotor dysfunction following traumatic brain injury in mice. J Neurosci Methods. 2003; 129:87–93. [PubMed: 12951236]

Blaiss CA, Yu TS, Zhang G, Chen J, Dimchev G, Parada LF, Powell CM, Kernie SG. Temporally specified genetic ablation of neurogenesis impairs cognitive recovery after traumatic brain injury. J Neurosci. 2011; 31:4906–4916. [PubMed: 21451029]

Borges FT, Reis LA, Schor N. Extracellular vesicles: structure, function, and potential clinical uses in renal diseases. Braz J Med Biol Res. 2013; 46:824–830. [PubMed: 24141609]

Braccioli L, van Velthoven C, Heijnen CJ. Exosomes: a new weapon to treat the central nervous system. Mol Neurobiol. 2014; 49:113–119. [PubMed: 23857502]

Chen J, Li Y, Wang L, Zhang Z, Lu D, Lu M, Chopp M. Therapeutic benefit of intravenous administration of bone marrow stromal cells after cerebral ischemia in rats. Stroke. 2001a; 32:1005–1011. [PubMed: 11283404]

Chen J, Sanberg PR, Li Y, Wang L, Lu M, Willing AE, Sanchez-Ramos J, Chopp M. Intravenous administration of human umbilical cord blood reduces behavioral deficits after stroke in rats. Stroke. 2001b; 32:2682–2688. [PubMed: 11692034]

Chen J, Zhang C, Jiang H, Li Y, Zhang L, Robin A, Katakowski M, Lu M, Chopp M. Atorvastatin induction of VEGF and BDNF promotes brain plasticity after stroke in mice. J Cereb Blood Flow Metab. 2005; 25:281–290. [PubMed: 15678129]

Chen J, Zhang ZG, Li Y, Wang L, Xu YX, Gautam SC, Lu M, Zhu Z, Chopp M. Intravenous administration of human bone marrow stromal cells induces angiogenesis in the ischemic boundary zone after stroke in rats. Circ Res. 2003; 92:692–699. [PubMed: 12609969]

Choi SH, Woodlee MT, Hong JJ, Schallert T. A simple modification of the water maze test to enhance daily detection of spatial memory in rats and mice. J Neurosci Methods. 2006; 156:182–193. [PubMed: 16621016]

Chopp M, Li Y. Treatment of neural injury with marrow stromal cells. Lancet Neurol. 2002; 1:92–100. [PubMed: 12849513]

Chopp M, Li Y, Zhang J. Plasticity and remodeling of brain. J Neurol Sci. 2008; 265:97–101. [PubMed: 17610903]

Cosme J, Liu PP, Gramolini AO. The cardiovascular exosome: current perspectives and potential. Proteomics. 2013; 13:1654–1659. [PubMed: 23526783]

Cox CS Jr. Baumgartner JE, Harting MT, Worth LL, Walker PA, Shah SK, Ewing-Cobbs L, Hasan KM, Day MC, Lee D, Jimenez F, Gee A. Autologous bone marrow mononuclear cell therapy for severe traumatic brain injury in children. Neurosurgery. 2011; 68:588–600. [PubMed: 21192274]

Cvjetkovic A, Lotvall J, Lasser C. The influence of rotor type and centrifugation time on the yield and purity of extracellular vesicles. J Extracell Vesicles. 2014:3.

Digirolamo CM, Stokes D, Colter D, Phinney DG, Class R, Prockop DJ. Propagation and senescence of human marrow stromal cells in culture: a simple colony-forming assay identifies samples with the greatest potential to propagate and differentiate. Br J Haematol. 1999; 107:275–281. [PubMed: 10583212]

Ding GL, Chopp M, Poulsen DJ, Li L, Qu C, Li Q, Nejad-Davarani SP, Budaj JS, Wu H, Mahmood A, Jiang Q. MRI of neuronal recovery after low-dose methamphetamine treatment of traumatic brain injury in rats. PLoS One. 2013; 8:e61241. [PubMed: 23637800]

Dixon CE, Clifton GL, Lighthall JW, Yaghmai AA, Hayes RL. A controlled cortical impact model of traumatic brain injury in the rat. J Neurosci Methods. 1991; 39:253–262. [PubMed: 1787745]

Doeppner TR, Hermann DM. Stem cell-based treatments against stroke: observations from human proof-of-concept studies and considerations regarding clinical applicability. Front Cell Neurosci. 2014; 8:357. [PubMed: 25400548]

Ekanger LA, Ali MM, Allen MJ. Oxidation-responsive Eu(2+/3+)-liposomal contrast agent for dual-mode magnetic resonance imaging. Chem Commun (Camb). 2014; 50:14835–14838. [PubMed: 25323054]

Ekdahl CT, Kokaia Z, Lindvall O. Brain inflammation and adult neurogenesis: the dual role of microglia. Neuroscience. 2009; 158:1021–1029. [PubMed: 18662748]

Gyorgy B, Szabo TG, Pasztoi M, Pal Z, Misjak P, Aradi B, Laszlo V, Pallinger E, Pap E, Kittel A, Nagy G, Falus A, Buzas EI. Membrane vesicles, current state-of-the-art: emerging role of extracellular vesicles. Cell Mol Life Sci. 2011; 68:2667–2688. [PubMed: 21560073]

Hailer NP. Immunosuppression after traumatic or ischemic CNS damage: it is neuroprotective and illuminates the role of microglial cells. Prog Neurobiol. 2008; 84:211–233. [PubMed: 18262323]

Ho AD, Wagner W, Franke W. Heterogeneity of mesenchymal stromal cell preparations. Cytotherapy. 2008; 10:320–330. [PubMed: 18574765]

Jin K, Sun Y, Xie L, Peel A, Mao XO, Batteur S, Greenberg DA. Directed migration of neuronal precursors into the ischemic cerebral cortex and striatum. Mol Cell Neurosci. 2003; 24:171–189. [PubMed: 14550778]

Joyce N, Annett G, Wirthlin L, Olson S, Bauer G, Nolta JA. Mesenchymal stem cells for the treatment of neurodegenerative disease. Regen Med. 2010; 5:933–946. [PubMed: 21082892]

Kalani A, Tyagi A, Tyagi N. Exosomes: mediators of neurodegeneration, neuroprotection and therapeutics. Mol Neurobiol. 2014; 49:590–600. [PubMed: 23999871]

Katsuda T, Kosaka N, Takeshita F, Ochiya T. The therapeutic potential of mesenchymal stem cell-derived extracellular vesicles. Proteomics. 2013; 13:1637–1653. [PubMed: 23335344]

Kernie SG, Parent JM. Forebrain neurogenesis after focal Ischemic and traumatic brain injury. Neurobiol Dis. 2010; 37:267–274. [PubMed: 19909815]

Kim DK, Nishida H, An SY, Shetty AK, Bartosh TJ, Prockop DJ. Chromatographically isolated CD63+CD81+ extracellular vesicles from mesenchymal stromal cells rescue cognitive impairments after TBI. Proc Natl Acad Sci U S A. 2016; 113:170–175. [PubMed: 26699510]

Kim HJ, Lee JH, Kim SH. Therapeutic effects of human mesenchymal stem cells on traumatic brain injury in rats: secretion of neurotrophic factors and inhibition of apoptosis. J Neurotrauma. 2010; 27:131–138. [PubMed: 19508155]

Kleindienst A, McGinn MJ, Harvey HB, Colello RJ, Hamm RJ, Bullock MR. Enhanced hippocampal neurogenesis by intraventricular S100B infusion is associated with improved cognitive recovery after traumatic brain injury. J Neurotrauma. 2005; 22:645–655. [PubMed: 15941374]

Lai RC, Chen TS, Lim SK. Mesenchymal stem cell exosome: a novel stem cell-based therapy for cardiovascular disease. Regen Med. 2011; 6:481–492. [PubMed: 21749206]

Lai RC, Yeo RW, Lim SK. Mesenchymal stem cell exosomes. Semin Cell Dev Biol. 2015; 40:82–88. [PubMed: 25765629]

Lai RC, Yeo RW, Tan KH, Lim SK. Mesenchymal stem cell exosome ameliorates reperfusion injury through proteomic complementation. Regen Med. 2013; 8:197–209. [PubMed: 23477399]

Lakshmipathy U, Hart RP. Concise review: MicroRNA expression in multipotent mesenchymal stromal cells. Stem Cells. 2008; 26:356–363. [PubMed: 17991914]

Lavoie JR, Rosu-Myles M. Uncovering the secretes of mesenchymal stem cells. Biochimie. 2013; 95:2212–2221. [PubMed: 23810910]

Li B, Mahmood A, Lu D, Wu H, Xiong Y, Qu C, Chopp M. Simvastatin attenuates microglial cells and astrocyte activation and decreases interleukin-1beta level after traumatic brain injury. Neurosurgery. 2009; 65:179–185. discussion 185-176. [PubMed: 19574840]

Li L, Chopp M, Ding GL, Qu CS, Li QJ, Lu M, Wang S, Nejad-Davarani SP, Mahmood A, Jiang Q. MRI measurement of angiogenesis and the therapeutic effect of acute marrow stromal cell administration on traumatic brain injury. J Cereb Blood Flow Metab. 2012; 32:2023–2032. [PubMed: 22781331]

Li L, Jiang Q, Zhang L, Ding G, Gang Zhang Z, Li Q, Ewing JR, Lu M, Panda S, Ledbetter KA, Whitton PA, Chopp M. Angiogenesis and improved cerebral blood flow in the ischemic boundary area detected by MRI after administration of sildenafil to rats with embolic stroke. Brain Res. 2007; 1132:185–192. [PubMed: 17188664]

Li Y, Chen J, Chen XG, Wang L, Gautam SC, Xu YX, Katakowski M, Zhang LJ, Lu M, Janakiraman N, Chopp M. Human marrow stromal cell therapy for stroke in rat: neurotrophins and functional recovery. Neurology. 2002; 59:514–523. [PubMed: 12196642]

Li Y, Chen J, Wang L, Lu M, Chopp M. Treatment of stroke in rat with intracarotid administration of marrow stromal cells. Neurology. 2001; 56:1666–1672. [PubMed: 11425931]

Li Y, Chopp M. Marrow stromal cell transplantation in stroke and traumatic brain injury. Neurosci Lett. 2009; 456:120–123. [PubMed: 19429146]

Liang X, Ding Y, Zhang Y, Tse HF, Lian Q. Paracrine mechanisms of Mesenchymal Stem cell-based therapy: Current status and perspectives. Cell Transplant. 2013

Liang X, Ding Y, Zhang Y, Tse HF, Lian Q. Paracrine mechanisms of mesenchymal stem cell-based therapy: current status and perspectives. Cell Transplant. 2014; 23:1045–1059. [PubMed: 23676629]

Lin B, Ginsberg MD, Zhao W, Alonso OF, Belayev L, Busto R. Quantitative analysis of microvascular alterations in traumatic brain injury by endothelial barrier antigen immunohistochemistry. J Neurotrauma. 2001; 18:389–397. [PubMed: 11336440]

Lo EH. A new penumbra: transitioning from injury into repair after stroke. Nat Med. 2008; 14:497–500. [PubMed: 18463660]

Lu D, Li Y, Wang L, Chen J, Mahmood A, Chopp M. Intraarterial administration of marrow stromal cells in a rat model of traumatic brain injury. J Neurotrauma. 2001a; 18:813–819. [PubMed: 11526987]

Lu D, Mahmood A, Goussev A, Schallert T, Qu C, Zhang ZG, Li Y, Lu M, Chopp M. Atorvastatin reduction of intravascular thrombosis, increase in cerebral microvascular patency and integrity, and enhancement of spatial learning in rats subjected to traumatic brain injury. J Neurosurg. 2004; 101:813–821. [PubMed: 15540920]

Lu D, Mahmood A, Qu C, Goussev A, Schallert T, Chopp M. Erythropoietin enhances neurogenesis and restores spatial memory in rats after traumatic brain injury. J Neurotrauma. 2005; 22:1011–1017. [PubMed: 16156716]

Lu D, Mahmood A, Qu C, Hong X, Kaplan D, Chopp M. Collagen scaffolds populated with human marrow stromal cells reduce lesion volume and improve functional outcome after traumatic brain injury. Neurosurgery. 2007; 61:596–602. discussion 602-593. [PubMed: 17881974]

Lu D, Mahmood A, Wang L, Li Y, Lu M, Chopp M. Adult bone marrow stromal cells administered intravenously to rats after traumatic brain injury migrate into brain and improve neurological outcome. Neuroreport. 2001b; 12:559–563. [PubMed: 11234763]

Mahmood A, Goussev A, Lu D, Qu C, Xiong Y, Kazmi H, Chopp M. Long-lasting benefits after treatment of traumatic brain injury (TBI) in rats with combination therapy of marrow stromal cells (MSCs) and simvastatin. J Neurotrauma. 2008; 25:1441–1447. [PubMed: 19072586]

Mahmood A, Lu D, Chopp M. Intravenous administration of marrow stromal cells (MSCs) increases the expression of growth factors in rat brain after traumatic brain injury. J Neurotrauma. 2004a; 21:33–39. [PubMed: 14987463]

Mahmood A, Lu D, Chopp M. Marrow stromal cell transplantation after traumatic brain injury promotes cellular proliferation within the brain. Neurosurgery. 2004b; 55:1185–1193. [PubMed: 15509325]

Mahmood A, Lu D, Qu C, Goussev A, Chopp M. Human marrow stromal cell treatment provides long-lasting benefit after traumatic brain injury in rats. Neurosurgery. 2005; 57:1026–1031. discussion 1026-1031. [PubMed: 16284572]

Mahmood A, Lu D, Qu C, Goussev A, Chopp M. Treatment of traumatic brain injury with a combination therapy of marrow stromal cells and atorvastatin in rats. Neurosurgery. 2007; 60:546–553. discussion 553-544. [PubMed: 17327800]

Mahmood A, Lu D, Wang L, Chopp M. Intracerebral transplantation of marrow stromal cells cultured with neurotrophic factors promotes functional recovery in adult rats subjected to traumatic brain injury. J Neurotrauma. 2002; 19:1609–1617. [PubMed: 12542861]

Mahmood A, Qu C, Ning R, Wu H, Goussev A, Xiong Y, Irtenkauf S, Li Y, Chopp M. Treatment of TBI with collagen scaffolds and human marrow stromal cells increases the expression of tissue plasminogen activator. J Neurotrauma. 2011; 28:1199–1207. [PubMed: 21355820]

Mahmood A, Wu H, Qu C, Mahmood S, Xiong Y, Kaplan D, Chopp M. Down-regulation of Nogo-A by collagen scaffolds impregnated with bone marrow stromal cell treatment after traumatic brain injury promotes axonal regeneration in rats. Brain Res. 2014a; 1542:41–48. [PubMed: 24177046]

Mahmood A, Wu H, Qu C, Mahmood S, Xiong Y, Kaplan DL, Chopp M. Suppression of neurocan and enhancement of axonal density in rats after treatment of traumatic brain injury with scaffolds impregnated with bone marrow stromal cells. J Neurosurg. 2014b; 120:1147–1155. [PubMed: 24460490]

Marklund N, Hillered L. Animal modelling of traumatic brain injury in preclinical drug development: where do we go from here? Br J Pharmacol. 2011; 164:1207–1229. [PubMed: 21175576]

Masyuk AI, Masyuk TV, Larusso NF. Exosomes in the pathogenesis, diagnostics and therapeutics of liver diseases. J Hepatol. 2013; 59:621–625. [PubMed: 23557871]

Meng Y, Xiong Y, Mahmood A, Zhang Y, Qu C, Chopp M. Dose-dependent neurorestorative effects of delayed treatment of traumatic brain injury with recombinant human erythropoietin in rats. J Neurosurg. 2011; 115:550–560. [PubMed: 21495821]

Morgan R, Kreipke CW, Roberts G, Bagchi M, Rafols JA. Neovascularization following traumatic brain injury: possible evidence for both angiogenesis and vasculogenesis. Neurol Res. 2007; 29:375–381. [PubMed: 17626733]

Morris RG, Garrud P, Rawlins JN, O'Keefe J. Place navigation impaired in rats with hippocampal lesions. Nature. 1982; 297:681–683. [PubMed: 7088155]

Narayan RK, Michel ME, Ansell B, Baethmann A, Biegon A, Bracken MB, Bullock MR, Choi SC, Clifton GL, Contant CF, Coplin WM, Dietrich WD, Ghajar J, Grady SM, Grossman RG, Hall ED, Heetderks W, Hovda DA, Jallo J, Katz RL, Knoller N, Kochanek PM, Maas AI, Majde J, Marion DW, Marmarou A, Marshall LF, McIntosh TK, Miller E, Mohberg N, Muizelaar JP, Pitts LH, Quinn P, Riesenfeld G, Robertson CS, Strauss KI, Teasdale G, Temkin N, Tuma R, Wade C,

Walker MD, Weinrich M, Whyte J, Wilberger J, Young AB, Yurkewicz L. Clinical trials in head injury. J Neurotrauma. 2002; 19:503–557. [PubMed: 12042091]

Nichols JE, Niles JA, Dewitt D, Prough D, Parsley M, Vega S, Cantu A, Lee E, Cortiella J. Neurogenic and neuro-protective potential of a novel subpopulation of peripheral blood-derived CD133+ ABCG2+CXCR4+ mesenchymal stem cells: development of autologous cell-based therapeutics for traumatic brain injury. Stem Cell Res Ther. 2013; 4:3. [PubMed: 23290300]

Ning R, Xiong Y, Mahmood A, Zhang Y, Meng Y, Qu C, Chopp M. Erythropoietin promotes neurovascular remodeling and long-term functional recovery in rats following traumatic brain injury. Brain Res. 2011; 1384:140–150. [PubMed: 21295557]

Nishibe M, Barbay S, Guggenmos D, Nudo RJ. Reorganization of motor cortex after controlled cortical impact in rats and implications for functional recovery. J Neurotrauma. 2010; 27:2221–2232. [PubMed: 20873958]

Ohab JJ, Fleming S, Blesch A, Carmichael ST. A neurovascular niche for neurogenesis after stroke. J Neurosci. 2006; 26:13007–13016. [PubMed: 17167090]

Pant S, Hilton H, Burczynski ME. The multifaceted exosome: biogenesis, role in normal and aberrant cellular function, and frontiers for pharmacological and biomarker opportunities. Biochem Pharmacol. 2012; 83:1484–1494. [PubMed: 22230477]

Parent JM, Vexler ZS, Gong C, Derugin N, Ferriero DM. Rat forebrain neurogenesis and striatal neuron replacement after focal stroke. Ann Neurol. 2002; 52:802–813. [PubMed: 12447935]

Paxinos, G., Watson, C. The rat brain in stereotaxic coordinates. 2nd. Academic Press; Sydney ; Orlando: 1986.

Peng W, Sun J, Sheng C, Wang Z, Wang Y, Zhang C, Fan R. Systematic review and meta-analysis of efficacy of mesenchymal stem cells on locomotor recovery in animal models of traumatic brain injury. Stem Cell Res Ther. 2015; 6:47. [PubMed: 25881229]

Qu C, Mahmood A, Liu XS, Xiong Y, Wang L, Wu H, Li B, Zhang ZG, Kaplan DL, Chopp M. The treatment of TBI with human marrow stromal cells impregnated into collagen scaffold: functional outcome and gene expression profile. Brain Res. 2011; 1371:129–139. [PubMed: 21062621]

Qu C, Mahmood A, Lu D, Goussev A, Xiong Y, Chopp M. Treatment of traumatic brain injury in mice with marrow stromal cells. Brain Res. 2008; 1208:234–239. [PubMed: 18384759]

Qu C, Xiong Y, Mahmood A, Kaplan DL, Goussev A, Ning R, Chopp M. Treatment of traumatic brain injury in mice with bone marrow stromal cell-impregnated collagen scaffolds. J Neurosurg. 2009; 111:658–665. [PubMed: 19425888]

Richardson RM, Sun D, Bullock MR. Neurogenesis after traumatic brain injury. Neurosurg Clin N Am. 2007; 18:169–181. xi. [PubMed: 17244562]

Schwab JM, Beschorner R, Nguyen TD, Meyermann R, Schluesener HJ. Differential cellular accumulation of connective tissue growth factor defines a subset of reactive astrocytes, invading fibroblasts, and endothelial cells following central nervous system injury in rats and humans. J Neurotrauma. 2001; 18:377–388. [PubMed: 11336439]

Simons M, Raposo G. Exosomes--vesicular carriers for intercellular communication. Curr Opin Cell Biol. 2009; 21:575–581. [PubMed: 19442504]

Singh S, Swarnkar S, Goswami P, Nath C. Astrocytes and microglia: responses to neuropathological conditions. Int J Neurosci. 2011; 121:589–597. [PubMed: 21827229]

Skolnick BE, Maas AI, Narayan RK, van der Hoop RG, MacAllister T, Ward JD, Nelson NR, Stocchetti N, Investigators ST. A clinical trial of progesterone for severe traumatic brain injury. N Engl J Med. 2014; 371:2467–2476. [PubMed: 25493978]

Smith JM, Lunga P, Story D, Harris N, Le Belle J, James MF, Pickard JD, Fawcett JW. Inosine promotes recovery of skilled motor function in a model of focal brain injury. Brain. 2007; 130:915–925. [PubMed: 17293357]

Sun D, McGinn MJ, Zhou Z, Harvey HB, Bullock MR, Colello RJ. Anatomical integration of newly generated dentate granule neurons following traumatic brain injury in adult rats and its association to cognitive recovery. Exp Neurol. 2007; 204:264–272. [PubMed: 17198703]

Sundholm-Peters NL, Yang HK, Goings GE, Walker AS, Szele FG. Subventricular zone neuroblasts emigrate toward cortical lesions. J Neuropathol Exp Neurol. 2005; 64:1089–1100. [PubMed: 16319719]

Swanson RA, Morton MT, Tsao-Wu G, Savalos RA, Davidson C, Sharp FR. A semiautomated method for measuring brain infarct volume. J Cereb Blood Flow Metab. 1990; 10:290–293. [PubMed: 1689322]

Taupin P. The therapeutic potential of adult neural stem cells. Curr Opin Mol Ther. 2006; 8:225–231. [PubMed: 16774042]

Taylor DD, Zacharias W, Gercel-Taylor C. Exosome isolation for proteomic analyses and RNA profiling. Methods Mol Biol. 2011; 728:235–246. [PubMed: 21468952]

Tsai MJ, Tsai SK, Hu BR, Liou DY, Huang SL, Huang MC, Huang WC, Cheng H, Huang SS. Recovery of neurological function of ischemic stroke by application of conditioned medium of bone marrow mesenchymal stem cells derived from normal and cerebral ischemia rats. J Biomed Sci. 2014; 21:5. [PubMed: 24447306]

Villarroya-Beltri C, Gutierrez-Vazquez C, Sanchez-Cabo F, Perez-Hernandez D, Vazquez J, Martin-Cofreces N, Martinez-Herrera DJ, Pascual-Montano A, Mittelbrunn M, Sanchez-Madrid F. Sumoylated hnRNPA2B1 controls the sorting of miRNAs into exosomes through binding to specific motifs. Nat Commun. 2013; 4:2980. [PubMed: 24356509]

Vlassov AV, Magdaleno S, Setterquist R, Conrad R. Exosomes: current knowledge of their composition, biological functions, and diagnostic and therapeutic potentials. Biochim Biophys Acta. 2012; 1820:940–948. [PubMed: 22503788]

Walker PA, Shah SK, Harting MT, Cox CS Jr. Progenitor cell therapies for traumatic brain injury: barriers and opportunities in translation. Dis Model Mech. 2009; 2:23–38. [PubMed: 19132123]

Walker PA, Shah SK, Jimenez F, Aroom KR, Harting MT, Cox CS Jr. Bone marrow-derived stromal cell therapy for traumatic brain injury is neuroprotective via stimulation of non-neurologic organ systems. Surgery. 2012; 152:790–793. [PubMed: 22853856]

Woodcock T, Morganti-Kossmann MC. The role of markers of inflammation in traumatic brain injury. Front Neurol. 2013; 4:18. [PubMed: 23459929]

Wright DW, Yeatts SD, Silbergleit R, Palesch YY, Hertzberg VS, Frankel M, Goldstein FC, Caveney AF, Howlett-Smith H, Bengelink EM, Manley GT, Merck LH, Janis LS, Barsan WG, Investigators N. Very early administration of progesterone for acute traumatic brain injury. N Engl J Med. 2014; 371:2457–2466. [PubMed: 25493974]

Xin H, Chopp M, Shen LH, Zhang RL, Zhang L, Zhang ZG, Li Y. Multipotent mesenchymal stromal cells decrease transforming growth factor beta1 expression in microglia/macrophages and down-regulate plasminogen activator inhibitor 1 expression in astrocytes after stroke. Neurosci Lett. 2013a; 542:81–86. [PubMed: 23499476]

Xin H, Li Y, Buller B, Katakowski M, Zhang Y, Wang X, Shang X, Zhang ZG, Chopp M. Exosome-mediated transfer of miR-133b from multipotent mesenchymal stromal cells to neural cells contributes to neurite outgrowth. Stem Cells. 2012; 30:1556–1564. [PubMed: 22605481]

Xin H, Li Y, Chopp M. Exosomes/miRNAs as mediating cell-based therapy of stroke. Front Cell Neurosci. 2014; 8:377. [PubMed: 25426026]

Xin H, Li Y, Cui Y, Yang JJ, Zhang ZG, Chopp M. Systemic administration of exosomes released from mesenchymal stromal cells promote functional recovery and neurovascular plasticity after stroke in rats. J Cereb Blood Flow Metab. 2013b; 33:1711–1715. [PubMed: 23963371]

Xin H, Li Y, Liu Z, Wang X, Shang X, Cui Y, Zhang ZG, Chopp M. MiR-133b promotes neural plasticity and functional recovery after treatment of stroke with multipotent mesenchymal stromal cells in rats via transfer of exosome-enriched extracellular particles. Stem Cells. 2013c; 31:2737–2746. [PubMed: 23630198]

Xiong Y, Mahmood A, Chopp M. Angiogenesis, neurogenesis and brain recovery of function following injury. Curr Opin Investig Drugs. 2010; 11:298–308.

Xiong Y, Mahmood A, Chopp M. Animal models of traumatic brain injury. Nat Rev Neurosci. 2013; 14:128–142. [PubMed: 23329160]

Xiong Y, Mahmood A, Meng Y, Zhang Y, Zhang ZG, Morris DC, Chopp M. Treatment of traumatic brain injury with thymosin beta(4) in rats. J Neurosurg. 2011a; 114:102–115. [PubMed: 20486893]

Xiong Y, Mahmood A, Zhang Y, Meng Y, Zhang ZG, Qu C, Sager TN, Chopp M. Effects of posttraumatic carbamylated erythropoietin therapy on reducing lesion volume and hippocampal

cell loss, enhancing angiogenesis and neurogenesis, and improving functional outcome in rats following traumatic brain injury. J Neurosurg. 2011b; 114:549–559. [PubMed: 21073254]

Xiong Y, Qu C, Mahmood A, Liu Z, Ning R, Li Y, Kaplan DL, Schallert T, Chopp M. Delayed transplantation of human marrow stromal cell-seeded scaffolds increases transcallosal neural fiber length, angiogenesis, and hippocampal neuronal survival and improves functional outcome after traumatic brain injury in rats. Brain Res. 2009; 1263:183–191. [PubMed: 19368838]

Xiong Y, Zhang Y, Mahmood A, Meng Y, Qu C, Chopp M. Erythropoietin mediates neurobehavioral recovery and neurovascular remodeling following traumatic brain injury in rats by increasing expression of vascular endothelial growth factor. Transl Stroke Res. 2011c; 2:619–632. [PubMed: 22707988]

Xu L, Yang BF, Ai J. MicroRNA transport: a new way in cell communication. J Cell Physiol. 2013; 228:1713–1719. [PubMed: 23460497]

Yu B, Zhang X, Li X. Exosomes derived from mesenchymal stem cells. Int J Mol Sci. 2014; 15:4142–4157. [PubMed: 24608926]

Zhang R, Liu Y, Yan K, Chen L, Chen XR, Li P, Chen FF, Jiang XD. Anti-inflammatory and immunomodulatory mechanisms of mesenchymal stem cell transplantation in experimental traumatic brain injury. J Neuroinflammation. 2013a; 10:106. [PubMed: 23971414]

Zhang R, Wang Y, Zhang L, Zhang Z, Tsang W, Lu M, Zhang L, Chopp M. Sildenafil (Viagra) induces neurogenesis and promotes functional recovery after stroke in rats. Stroke. 2002; 33:2675–2680. [PubMed: 12411660]

Zhang Y, Chopp M, Mahmood A, Meng Y, Qu C, Xiong Y. Impact of inhibition of erythropoietin treatment-mediated neurogenesis in the dentate gyrus of the hippocampus on restoration of spatial learning after traumatic brain injury. Exp Neurol. 2012; 235:336–344. [PubMed: 22414310]

Zhang Y, Chopp M, Meng Y, Katakowski M, Xin H, Mahmood A, Xiong Y. Effect of exosomes derived from multipluripotent mesenchymal stromal cells on functional recovery and neurovascular plasticity in rats after traumatic brain injury. J Neurosurg. 2015; 122:856–867. [PubMed: 25594326]

Zhang Y, Chopp M, Meng Y, Zhang ZG, Doppler E, Mahmood A, Xiong Y. Improvement in functional recovery with administration of Cerebrolysin after experimental closed head injury. J Neurosurg. 2013b; 118:1343–1355. [PubMed: 23581594]

Zhang ZG, Chopp M. Promoting brain remodeling to aid in stroke recovery. Trends Mol Med. 2015; 21:543–548. [PubMed: 26278490]

Zhang ZG, Chopp M. Exosomes in stroke pathogenesis and therapy. J Clin Invest. 2016; 126:1190–1197. [PubMed: 27035810]

Zhang ZX, Guan LX, Zhang K, Zhang Q, Dai LJ. A combined procedure to deliver autologous mesenchymal stromal cells to patients with traumatic brain injury. Cytotherapy. 2008; 10:134–139. [PubMed: 18368592]

Zheng W, ZhuGe Q, Zhong M, Chen G, Shao B, Wang H, Mao X, Xie L, Jin K. Neurogenesis in adult human brain after traumatic brain injury. J Neurotrauma. 2013; 30:1872–1880. [PubMed: 21275797]

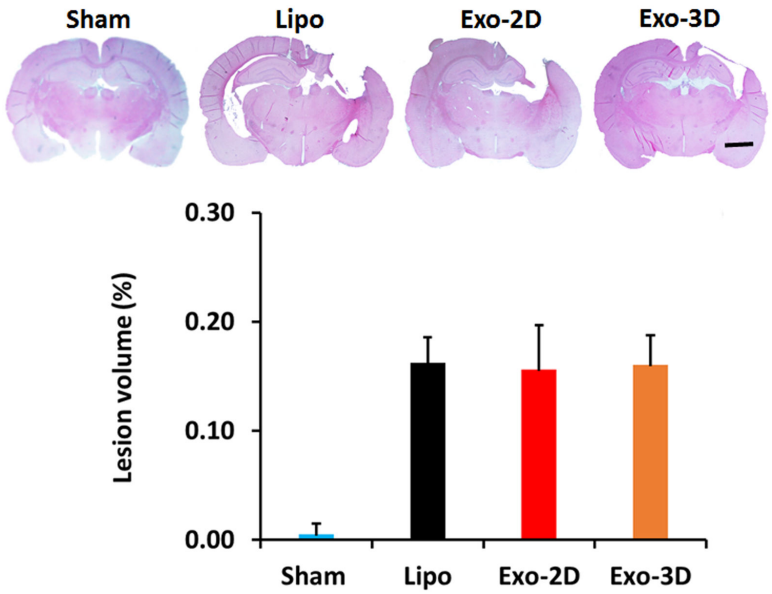

Fig. 1.

Effect of treatment with exosomes derived from hMSCs on cortical lesion volume examined 35 days after TBI. TBI caused significant cortical tissue loss in the liposome-treated rats. The bar graph showing that exosome treatments did not reduce lesion volume compared to the liposome-treated groups ($p > 0.05$). Scale bar = 3 mm. Data represent mean ± SD. N = 8/group.

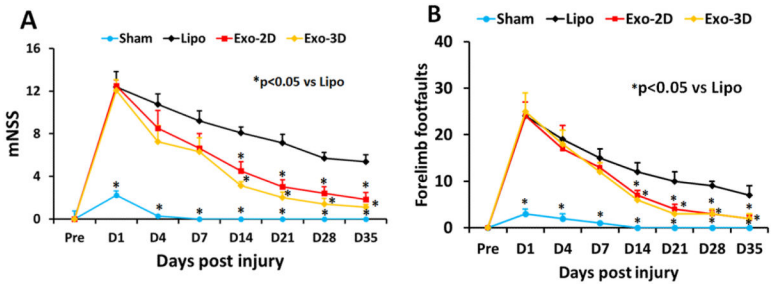

Fig. 2.

Treatment with exosomes derived from hMSCs significantly improves sensorimotor functional recovery measured by mNSS (**A**), and right forelimb footfault test (**B**) in rats after TBI. *p < 0.05 vs liposome group. Data represent mean ± SD. N = 8/group.

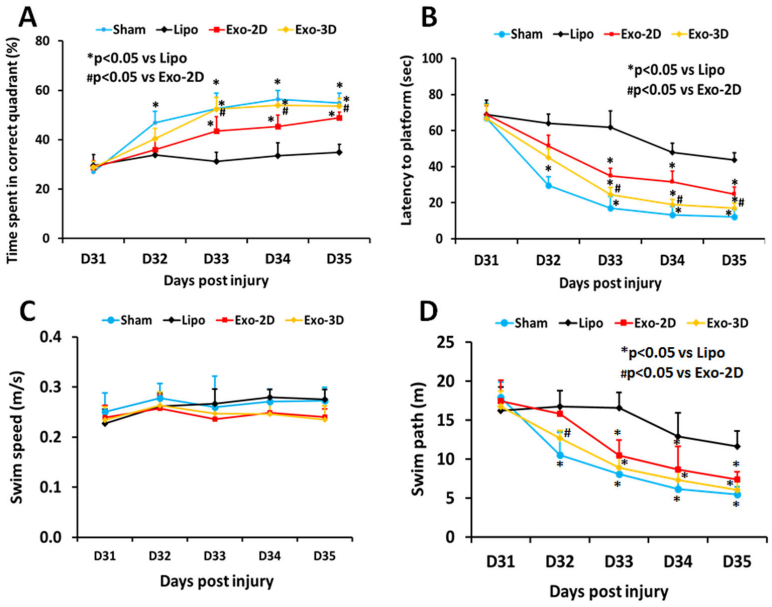

Fig. 3.

Treatment with exosomes derived from hMSCs significantly improves spatial lerning in the Morris water maze test measured by percentage time spent (**A**), and latency to find the hidden platform (**B**) in the correct quadrant by rats after TBI. There was no significant difference in the swim speeds between groups (C). However, swim path lengths for the liposome-treated TBI rats were significantly greater than those for Sham rats and Exo-2D and Exo-3D-treated TBI rats (D). *p < 0.05 vs Lipo group. #p < 0.05 vs Exo-2D group. Data represent mean ± SD. N = 8/group.

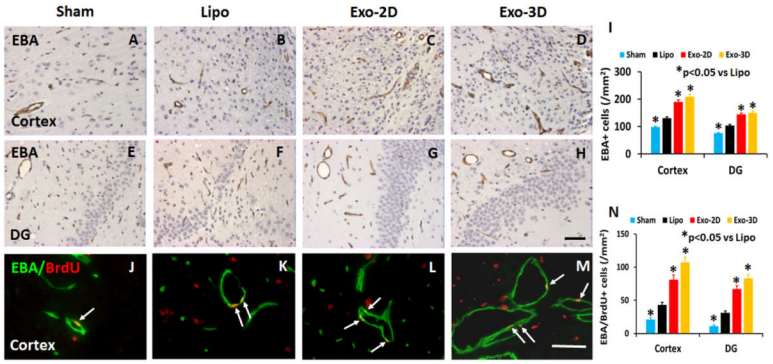

Fig. 4.

Treatment with exosomes derived from hMSCs significantly increases brain vascular density and angiogenesis in rats after TBI. EBA staining was performed for detection of mature vasculature at day 35 after TBI in the lesion boundary zone and dentate gyrus (DG) from rat brains in the sham group (**A** and **E**), liposome-treated group (**B** and **F**), and exosome-treated groups (**C and G** for Exo-2D**; D and H** for Exo-3D). Double staining for EBA (green) and BrdU (red) to identify newly formed mature vessels (arrows, **J-M**) in the brain at day 35 after TBI. Scale bar (**F, J**) =25 μm. Data in bar graph (**I, N**) represent mean ± SD. *p < 0.05 vs liposome group. N = 8/group.

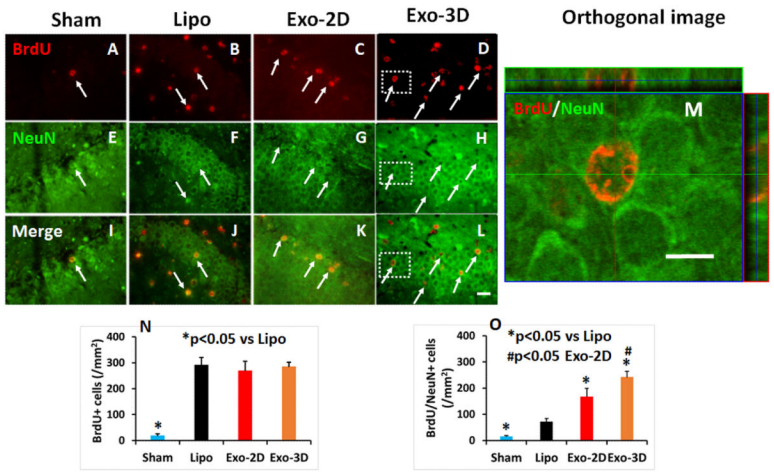

Fig. 5.

Treatment with exosomes derived from hMSCs significantly increases neurogenesis in the DG of rats sacrificed at day 35 after TBI. Double staining with BrdU (red, **A-D**)/NeuN (green, **E-H**) was performed to identify newborn mature neurons indicated by yellow arrows (**I-L**, arrows). The orthogonal view (**M**) from the insert of L (white box) shows co-localization for a BrdU+ cell with NeuN. Scale bar = 25 μm (**L**), 10 μm (**M**). Data in bar graphs **N, O**) represent mean ± SD. *p < 0.05 vs liposome group. #p < 0.05 vs Exo-2D group. N = 8/group.

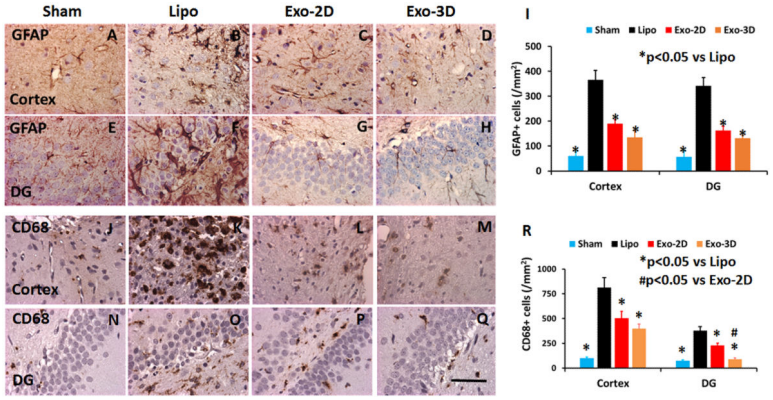

Fig. 6.

Treatment with exosomes derived from hMSCs significantly reduces the number of activated GFAP+ astrocytes and CD68+ microglia/macrophages in the brain of rats sacrificed at day 35 after TBI. GFAP staining for reactive astrocytes (**A-H)**. CD68 staining for activated microglia/macrophages (**J-Q**). Scale bar = 50 μm (**Q**). Data in bar graphs (**I, R**) represent mean ± SD. N = 8/group.